Aerospace Science and Technology 68 (2017) 149–162

Contents lists available at ScienceDirect

Aerospace Science and Technology

www.elsevier.com/locate/aescte

A health evaluation method of multicopters modeled by Stochastic Hybrid System ☆

Zhiyao Zhao [a,b,*], Quan Quan [a], Kai-Yuan Cai [a]

[a] School of Automation Science and Electrical Engineering, Beihang University, Beijing 100191, China
[b] School of Computer and Information Engineering, Beijing Technology and Business University, Beijing 100048, China

A R T I C L E I N F O

Article history:
Received 25 January 2016
Received in revised form 29 January 2017
Accepted 4 May 2017
Available online 10 May 2017

Keywords:
Health evaluation
Multicopter
Stochastic Hybrid System
Interacting multiple model
Health degree
Sensor anomaly

A B S T R A C T

For multicopters, failures may abort missions, crash multicopters, and moreover, injure or even kill people. In order to guarantee flight safety, a system of prognostics and health management should be designed to prevent or mitigate unsafe consequences of multicopter failures, where health evaluation is an indispensable module. This paper proposes a health evaluation method of multicopters based on Stochastic Hybrid System (SHS). In the SHS model, different working conditions (health statuses) of multicopters are modeled as discrete states, and system behaviors of different working conditions are modeled as continuous dynamics under discrete states. Then, the health of multicopters is quantitatively measured by a definition of health degree, which is a probability measure describing an extent of system degradation from an expected normal condition. On this basis, the problem of multicopter's health evaluation is transformed to a hybrid state estimation problem. In this case, a modified interacting-multiple-model algorithm is proposed to estimate the real-time distribution of hybrid state, and evaluate multicopter's health. Finally, a case study of multicopter with sensor anomalies is presented to validate the effectiveness of the proposed method.

1. Introduction

1.1. Motivation and outline

Multicopters have attracted close attention in the field of aircraft engineering. They are well-suited to a wide range of mission scenarios, such as search and rescue [1,2], package delivery [3], border patrol [4], military surveillance [3,5] and agricultural application [6,7]. From a safety perspective, multicopter failures cannot be absolutely avoided, including communication breakdown, sensor failure and propulsion system anomaly, etc. These failures may abort missions, crash multicopters, and moreover, injure or even kill people. In order to guarantee flight safety, a system of Prognostics and Health Management (PHM) should be designed to prevent or mitigate unsafe consequences caused by multicopter failures [8]. As shown in Fig. 1, health evaluation is a key component in the PHM system, which has been highly concerned in the field of system engineering [9–12]. Information obtained from health evaluation can be used to understand the system behavior, also as a reference for operating a safety decision-making [13].

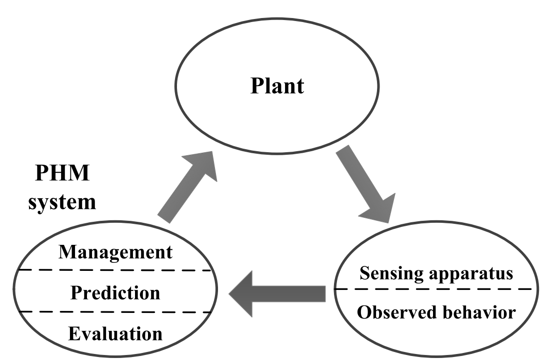

Fig. 1. PHM framework.

The current research of health evaluation commonly focuses on a component level [14]. Fault diagnosis [15–19] and fault-tolerant control [20–25] related to specific components have been extensively studied for enhancing the flight safety of aircrafts. Different from fault diagnosis, health evaluation research should concentrate on a performance of the whole aircraft rather than a fault occurred in local onboard components [12,26]. For multicopters, different onboard components such as actuators and sensors are correlated

☆ This work is supported by the National Natural Science Foundation of China (Grant No. 61473012, No. 51179002 and No. 61603014).
* Corresponding author.
E-mail addresses: zzy_buaa@buaa.edu.cn (Z. Zhao), qq_buaa@buaa.edu.cn (Q. Quan), kycai@buaa.edu.cn (K.-Y. Cai).

http://dx.doi.org/10.1016/j.ast.2017.05.011
1270-9638/© 2017 Published by Elsevier Masson SAS.

Notation

$\boldsymbol{x}$	Process variable vector	$H(\cdot)$	Health degree
$\boldsymbol{y}$	Observation	$\mathcal{P}\{\cdot\}$	Probability measure
p_x, p_y, p_z	Multicopter's position in the earth-fixed frame	Tr	Mission trajectory
$\boldsymbol{w}, \boldsymbol{\Gamma_w}, \mathbf{Q}$	Process noise, its covariance matrix and driven matrix	$\boldsymbol{\Pi}$	Transition probability matrix
$\boldsymbol{v}, \boldsymbol{\Gamma_v}, \mathbf{R}$	Measurement noise, its covariance matrix and driven matrix	π	Transition probability
q	Discrete state	$\hat{\boldsymbol{x}}$	Estimate of $\boldsymbol{x}$
$f(\cdot)$	Probability density distribution	$\mathbf{P}$	Covariance matrix of $\boldsymbol{x}$
		T	Sample time
		$\mathcal{N}(\cdot)$	Gaussian distribution

through the autopilot. Sensor measurements are sent to the autopilot, analyzed in the autopilot, and then the control instructions are sent to actuators from the autopilot. In this case, the health of multicopters cannot only consider onboard component faults, but also the whole system behavior directed by the autopilot. However, there is little study concerning multicopter's health evaluation from a system behavior perspective. The main reason lies in two aspects: 1) a quantitative definition of system health is lacked. Residuals are always viewed as a quantitative index to characterize a fault [27–30] in fault diagnosis research, while PHM research always uses different kinds of physical and mathematical quantities as health indicators, such as sensor measurements [31,32], features [33,34] and reliability indices [35–38]. However, a unified mathematical definition to describe and quantitatively measure system health is lacked and required to be proposed. 2) A multicopter model for both health evaluation and safety decision-making research is lacked. The current research always separately studied health evaluation and safety decision-making of multicopters by using different models. Actually, accurate health evaluation is a key premise of correct safety decision-making, while safety decision-making is the final purpose of health evaluation. Thus, it is required to study a model which can be used for both health evaluation and safety decision-making research.

Stochastic Hybrid System (SHS) can be used to analyze and design complex systems that operate in the presence of uncertainties, and contain multiple working modes [39–41]. It can model multicopter's dynamic behavior and performance degradation, because it interacts continuous dynamics and discrete dynamics [42,43]. These characteristics enable SHS to be used in designing multicopter's autopilot for the purpose of both health evaluation and safety decision-making. In this case, this paper proposes an SHS-based health evaluation method for multicopters. In the SHS model, different working conditions (health statuses) of multicopters are modeled as discrete states, and system behaviors of different working conditions are modeled as continuous dynamics under discrete states. Then, the health of multicopters is quantitatively measured by a definition of health degree, which is a probability measure describing an extent of system degradation from an expected normal condition. On this basis, the problem of multicopter's health evaluation is transformed to a hybrid state estimation problem. In this case, a modified interacting-multiple-model (IMM) algorithm is proposed to estimate the real-time distribution of hybrid state, and the health degree is further calculated. Finally, a case study of a multicopter with sensor anomalies is simulated to validate the effectiveness of the proposed method, and some comparative studies are also made and discussed.

1.2. Related work

The UAV health can be characterized into four categories [14]:

1) Structure/Actuator health. This category focuses on damage of structure and actuator components of UAVs. For structure health, flight data and vibration signals from airframe including wings [44,45], blades [46] and tail booms [47] are usually collected and analyzed by data-driven approaches to detect anomalies in both time and frequency domain [48]. For actuator health, filtering-based methods are always used to estimate an additive fault [49,50] or a degradation of control efficiency [51], where residuals [27–30] and controllability index [52] are viewed as health indices. On this basis, fault-tolerant algorithms dealt with such failures [20–25] are widely studied.

2) Sensor health. This category focuses on failure of onboard sensor-hardwares such as barometers, gyroscopes, etc. Sensor failure may include loss of signal, signal stuck, drift, big noise interference, etc. Similar as actuators, the health evaluation of sensors can be also based on observers and filtering-based methods [53–55]. Meanwhile, data-driven approaches [56] and fusion approaches [57,58] are also proposed to detect sensor faults. Based on fault detection results, fault-tolerant algorithms dealt with such a failure [59,60] are also studied.

3) Communication health. This category concentrates on the functionality of the signal transmission between the UAV and the remote controller or ground control station, even among multiple UAVs. Interference, loss of contact and degraded contact quality are commonly appeared during flight. In this area, most works study the decision-making, coordination and cooperation of a UAV team when communication anomaly occurs [61]. Meanwhile, there exists research about mission planning for communication constraint situation [5]. In addition, civilian-purposed UAVs are vulnerable to malicious data interference. This leads to a game-theoretical analysis of attack and anti-attack of UAVs by using communication channels [62–64].

4) Fuel health. Battery is commonly-seen as a power source of small UAVs. State-of charge and state-of-health are two indices reflecting the remaining capacity and residual life of batteries [65]. There exists amounts of research on the evaluation and prediction of these indices [66–69]. For safety and reliability purpose, battery management system is also studied and developed [70–72]. For other type of fuel, the emphasis is on the mission planning when the fuel quantity drops below a certain threshold [73,74].

To sum up, the existed PHM methods of UAVs are mainly focused on the fault detection and identification at the component level and the corresponding mission planning scheme. In these methods, sensor measurements, features, residuals and reliability indices are used as health indicators. Different from the mentioned research, this paper introduces a concept of health degree as a unified health indicator to evaluate health of multicopters, where the value quantitatively reflects the performance deviation from the expected normal condition. Since the health degree is calculated based on the distribution of system process (continuous) variables, the proposed method is a health evaluation method at a system behavior level.

The remainder of this paper is organized as follows. Section 2 proposes an SHS-based model of multicopters, and quantitatively defines its health by introducing the definition of health degree. Section 3 proposes a modified IMM algorithm to evaluate the health of the multicopter. Section 4 presents a case study of multicopter with sensor anomalies to validate the effectiveness and advantages of the proposed health evaluation method, where simulation results are given and discussed. Section 5 gives a conclusion, and indicates future development of the proposed method.

2. An SHS-based modeling of multicopter and its health definition

In this section, preliminaries of discrete-time SHS model [40–43] are presented. Then, two kinds of models, namely "Stochastic Continuous System (SCS)-based model" and "SHS-based model", are presented to model the multicopter for the purpose of health evaluation. On this basis, a health definition of multicopters is proposed.

2.1. Preliminaries

Let $(\Omega, \mathcal{F}, \mathcal{F}_t, \mathcal{P})$ be a complete probability space with a sample space Ω, a σ-field of the events $\mathcal{F}$, a natural filtration $\mathcal{F}_t$ and a natural probability measure $\mathcal{P}:\mathcal{F} \longrightarrow [0,1]$. Let $\mathcal{B}(\cdot)$ denote the Borel σ-algebra.

Definition 1. In the probability space $(\Omega, \mathcal{F}, \mathcal{F}_t, \mathcal{P})$, a general discrete-time SHS model is a tuple $\mathcal{H} = \left(\mathcal{Q}, n, Init, T_x, T_q, R\right)$, which is detailed as follows:

1) $\mathcal{Q} := \{q_1, q_2, \cdots, q_m\}$ is a finite set of discrete states for $m \in \mathbb{N}$.

2) $n : \mathcal{Q} \longrightarrow \mathbb{N}$ which assigns each discrete state $q \in \mathcal{Q}$ a continuous state space $\mathbb{R}^{n(q)}$. Then, the hybrid state $\boldsymbol{s} = (q, \boldsymbol{x})$ is defined in the hybrid state space $\mathcal{S} = \mathcal{Q} \times \mathbb{R}^{n(q)}$.

3) $Init : \mathcal{B}(\mathcal{S}) \longrightarrow [0,1]$ represents the initial distribution of the hybrid state space $\mathcal{S}$.

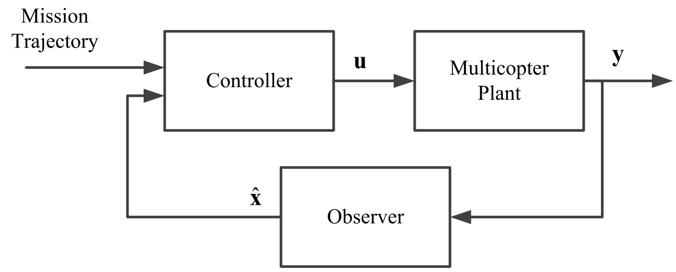

Fig. 2. General closed-loop multicopter model.

4) $T_x : \mathcal{B}\left(\mathbb{R}^{n(\cdot)}\right) \times \mathcal{S} \longrightarrow [0,1]$ is a Borel-measurable stochastic kernel on $\mathbb{R}^{n(\cdot)}$ given $\mathcal{S}$, which assigns to each $\boldsymbol{s} \in \mathcal{S}$ a probability measure on the Borel space $\left(\mathbb{R}^{n(q)}, \mathcal{B}\left(\mathbb{R}^{n(q)}\right)\right) : T_x\left(\cdot\,|\boldsymbol{s}\right)$.

5) $T_q : \mathcal{Q} \times \mathcal{S} \longrightarrow [0,1]$ is a discrete stochastic kernel on $\mathcal{Q}$ given $\mathcal{S}$, which assigns to each $\boldsymbol{s} \in \mathcal{S}$ a probability distribution over $\mathcal{Q} : T_q\left(\cdot\,|\boldsymbol{s}\right)$.

6) $R : \mathcal{B}\left(\mathbb{R}^{n(\cdot)}\right) \times \mathcal{S} \times \mathcal{Q} \longrightarrow [0,1]$ is a Borel-measurable stochastic kernel on $\mathbb{R}^{n(\cdot)}$ given $\mathcal{S} \times \mathcal{Q}$, that assigns to each $\boldsymbol{s} \in \mathcal{S}$, and $q' \in \mathcal{Q}$ a probability measure on the Borel space $\left(\mathbb{R}^{n(q')}, \mathcal{B}\left(\mathbb{R}^{n(q')}\right)\right)$ $: R\left(\cdot\,|\boldsymbol{s}, q'\right)$.

2.2. Multicopter modeling

In this section, two kinds of closed-loop multicopter models including multicopter plant, controller, and observer are presented. Fig. 2 describes a general framework of the multicopter model, while Fig. 3 presents the "multicopter plant" in Fig. 2. The details of the two models are presented as follows.

2.2.1. SCS-based model

Scholars have studied the dynamics of multicopters [49,50, 75–77]. Equation (1) presents a general dynamic model:

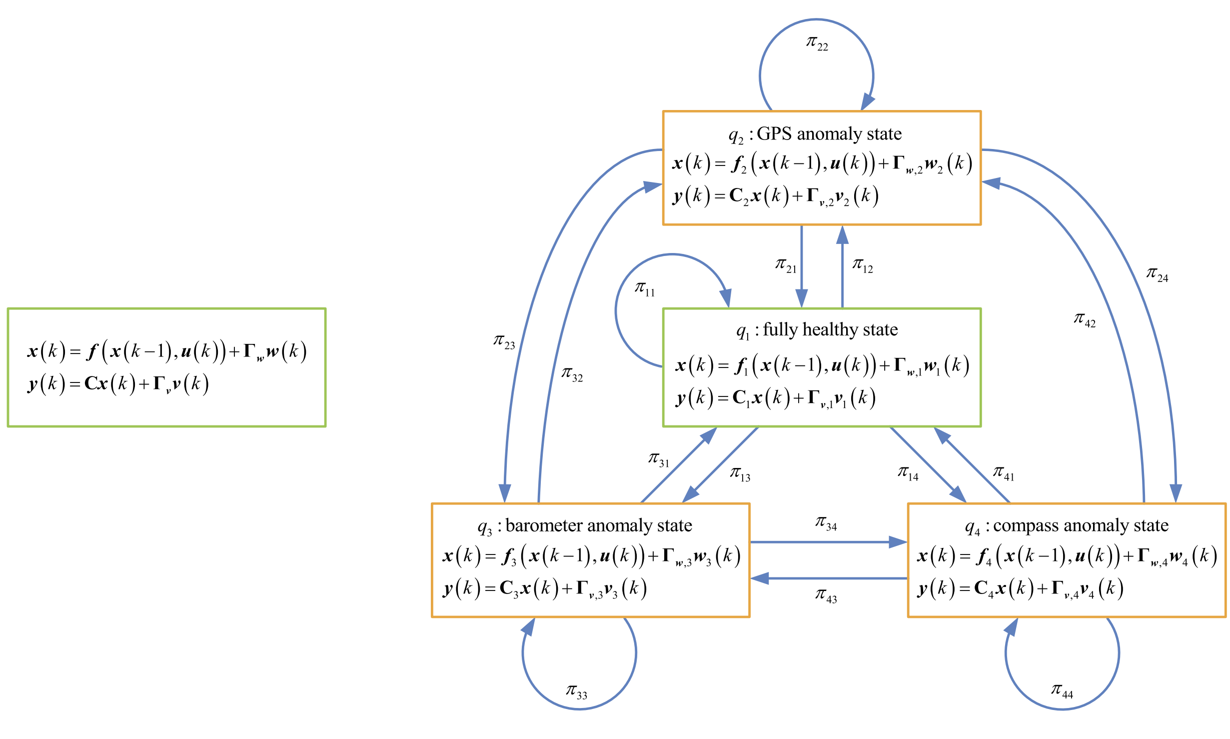

(a) SCS-based model plant (b) SHS-based model plant

Fig. 3. Model plant.

$$\underbrace{\begin{array}{l}\dot{p}_x = v_x \\ \dot{p}_y = v_y \\ \dot{p}_z = v_z \\ \dot{v}_x = -u_z\left(\cos\phi\sin\theta\cos\psi + \sin\phi\sin\psi\right)/m \\ \dot{v}_y = -u_z\left(\cos\phi\sin\theta\sin\psi - \sin\phi\cos\psi\right)/m \\ \dot{v}_z = -u_z\cos\phi\cos\theta/m + g \\ \dot{\phi} = v_\phi + \tan\theta\left(v_\psi\cos\phi + v_\theta\sin\phi\right) \\ \dot{\theta} = v_\theta\cos\phi - v_\psi\sin\phi \\ \dot{\psi} = \sec\theta\left(v_\psi\cos\phi + v_\theta\sin\phi\right) \\ \dot{v}_\phi = \left(J_y - J_z\right)v_\psi v_\theta/J_x + u_\phi/J_x \\ \dot{v}_\theta = \left(J_z - J_x\right)v_\phi v_\psi/J_y + u_\theta/J_y \\ \dot{v}_\psi = \left(J_x - J_y\right)v_\phi v_\theta/J_z + u_\psi/J_z \end{array}}_{\dot{\boldsymbol{x}} = \mathbf{G}(\boldsymbol{x},\boldsymbol{u})} \tag{1}$$

where the vector $\boldsymbol{x} = \left(p_x, p_y, p_z, v_x, v_y, v_z, \phi, \theta, \psi, v_\phi, v_\theta, v_\psi\right)^{\mathrm{T}} \in \mathbb{R}^{12\times 1}$ contains process variables of the multicopter. The components p_x, p_y, p_z represent the multicopter's position in the earth-fixed frame; the components v_x, v_y, v_z represent the multicopter's velocity in the earth-fixed frame; the components ϕ, θ, ψ represent the angles of roll, pitch and yaw, respectively; the components v_ϕ, v_θ, v_ψ represent the angular velocity of ϕ, θ, ψ, respectively; The parameters J_x, J_y, J_z are the moments of inertia along x, y, z directions, respectively; m is the mass of the multicopter; g is the acceleration of gravity. The positive direction of z-axis of the earth-fixed frame points to the ground. The control input $\boldsymbol{u} = \left[u_z, u_\phi, u_\theta, u_\psi\right]^{\mathrm{T}}$ includes a total lift and moments of angles ϕ, θ, ψ, respectively.

With the estimated $\hat{\boldsymbol{x}}$ by a designed observer and an expected control target $\boldsymbol{x}_d = \left[p_{x,d}, p_{y,d}, p_{z,d}, \psi_d\right]^{\mathrm{T}}$, the control input $\boldsymbol{u} = \left[u_z, u_\phi, u_\theta, u_\psi\right]^{\mathrm{T}}$ can be calculated by a PD controller as

$$\begin{aligned} u_z &= -k_{P,z}\left(p_{z,d} - \hat{p}_z\right) + k_{D,z}\hat{v}_z + mg \\ u_\phi &= k_{P,\phi}\left(\phi_d - \hat{\phi}\right) - k_{D,\phi}\hat{v}_\phi \\ u_\theta &= k_{P,\theta}\left(\theta_d - \hat{\theta}\right) - k_{D,\theta}\hat{v}_\theta \\ u_\psi &= k_{P,\psi}\left(\psi_d - \hat{\psi}\right) - k_{D,\psi}\hat{v}_\psi, \end{aligned} \tag{2}$$

where

$$\begin{bmatrix}\theta_d \\ \phi_d\end{bmatrix} = g^{-1}\begin{pmatrix}\cos\hat{\psi} & \sin\hat{\psi} \\ \sin\hat{\psi} & -\cos\hat{\psi}\end{pmatrix}^{-1} \times \left(\mathbf{K}_{Pa}\begin{bmatrix}\hat{p}_x - p_{x,d} \\ \hat{p}_y - p_{y,d}\end{bmatrix} + \mathbf{K}_{Da}\begin{bmatrix}\hat{v}_x \\ \hat{v}_y\end{bmatrix}\right). \tag{3}$$

Equations (2) and (3) describe a position controller of the multicopter. To obtain the discrete-time dynamic model of the multicopter, equation (1) is discretized through the Euler method [78] as

$$\boldsymbol{x}(k) = \boldsymbol{x}(k-1) + T\mathbf{G}\left(\boldsymbol{x}(k-1), \boldsymbol{u}(k)\right), \tag{4}$$

where T is the discretized time. Combining (4) with an observation equation and related noise items, we have

$$\begin{aligned} \boldsymbol{x}(k) &= \boldsymbol{f}\left(\boldsymbol{x}(k-1), \boldsymbol{u}(k)\right) + \boldsymbol{\Gamma}_{\boldsymbol{w}}\boldsymbol{w}(k) \\ \boldsymbol{y}(k) &= \mathbf{C}\boldsymbol{x}(k) + \boldsymbol{\Gamma}_{\boldsymbol{v}}\boldsymbol{v}(k) \end{aligned} \tag{5}$$

where the function $\boldsymbol{f}\left(\boldsymbol{x}(k-1), \boldsymbol{u}(k)\right) = \boldsymbol{x}(k-1) + T\mathbf{G}(\boldsymbol{x}(k-1), \boldsymbol{u}(k))$; the vector $\boldsymbol{y}$ contains system measurements, and $\mathbf{C}$ is the corresponding parameter matrix. Without loss of generality, let $\mathbf{C} = \mathbf{I}_{12}$ be an identity matrix, which means all process variables are directly measured. The items $\boldsymbol{w}$ and $\boldsymbol{v}$ are the process noise and measurement noise, satisfying that

$$\begin{cases} \boldsymbol{w}(\cdot) \sim \mathcal{N}(\mathbf{0}, \mathbf{Q}), \boldsymbol{v}(\cdot) \sim \mathcal{N}(\mathbf{0}, \mathbf{R}), \forall k \\ \operatorname{cov}\left[\boldsymbol{w}(k), \boldsymbol{v}(j)\right] = E\left[\boldsymbol{w}(k)\boldsymbol{v}^T(j)\right] = \mathbf{0}, \forall k, j \end{cases}, \tag{6}$$

where $\mathbf{Q}$ and $\mathbf{R}$ are the covariance matrices. The matrices $\boldsymbol{\Gamma}_{\boldsymbol{w}}$ and $\boldsymbol{\Gamma}_{\boldsymbol{v}}$ are the corresponding noise driven matrices. Note that equation (5) is a discrete-time stochastic continuous (variable) system.

Remark 1. The presented model in this part, namely "SCS-based model", only models the multicopter system when the multicopter is in a fully healthy status. However, for the purpose of health evaluation, the multicopter contains different health statuses, where transitions might occur among them. Considering the SHS model has discrete dynamics as well as continuous dynamics, an SHS-based multicopter is presented for the purpose of health evaluation.

2.2.2. SHS-based model

An SHS-based multicopter model is constructed as shown in Fig. 3(b). For simplicity, we have two assumptions as follows.

Assumption 1. *Sensors including GPS, barometer and compass are considered to be possibly unhealthy in the SHS-based model. The other onboard components such as propulsion system, communication system and other sensors are all considered to be healthy.*

Assumption 2. *There will be at most one anomaly occurred in either GPS, barometer or compass at the same time, which means it is impossible that two sensors are simultaneously unhealthy.*

Remark 2. Assumption 1 confines the discrete dimension of the SHS-based model, which leads to convenient understanding of the SHS-based model structure and the subsequent health evaluation algorithm. Assumption 2 also confines the discrete dimension. This is reasonable, because there is little chance that two sensors are both unhealthy at the same time for a qualified multicopter product. Actually, Assumptions 1 and 2 can be relaxed by introducing more discrete states of SHS (health statuses). This relaxation has little influence on the health evaluation algorithm.

According to Assumptions 1 and 2, four discrete states are considered in the SHS-based multicopter model. Following Definition 1, we have

$$\mathcal{Q} = \{q_1, q_2, q_3, q_4\},$$

where q_1 is a fully healthy status, q_2 is a GPS anomaly status, q_3 is a barometer anomaly status, and q_4 is a compass anomaly status, respectively. For $\forall q_j \in \mathcal{Q}$, the continuous dynamics is

$$\begin{aligned} \boldsymbol{x}(k) &= \boldsymbol{f}_j\left(\boldsymbol{x}(k-1), \boldsymbol{u}(k)\right) + \boldsymbol{\Gamma}_{\boldsymbol{w},j}\boldsymbol{w}_j(k) \\ \boldsymbol{y}(k) &= \mathbf{C}_j\boldsymbol{x}(k) + \boldsymbol{\Gamma}_{\boldsymbol{v},j}\boldsymbol{v}_j(k) \end{aligned}, \tag{7}$$

where

$$\begin{cases} \boldsymbol{f}_1(\cdot) = \boldsymbol{f}_2(\cdot) = \boldsymbol{f}_3(\cdot) = \boldsymbol{f}_4(\cdot) = \boldsymbol{f} \\ \boldsymbol{\Gamma}_{\boldsymbol{w},1} = \boldsymbol{\Gamma}_{\boldsymbol{w},2} = \boldsymbol{\Gamma}_{\boldsymbol{w},3} = \boldsymbol{\Gamma}_{\boldsymbol{w},4} = \boldsymbol{\Gamma}_{\boldsymbol{w}} \\ f(\boldsymbol{w}_1) = f(\boldsymbol{w}_2) = f(\boldsymbol{w}_3) = f(\boldsymbol{w}_4) = f(\boldsymbol{w}) \end{cases}.$$

The symbol $f(\boldsymbol{w})$ is the probability density function (pdf) of $\boldsymbol{w}$. Note that $\boldsymbol{f}_j(\cdot)$ contains the controller same as (2). As to the observation equation, for state q_1, we have

$$\begin{cases} \mathbf{C}_1 = \begin{bmatrix}\boldsymbol{c}_1 \\ \boldsymbol{c}_2 \\ \vdots \\ \boldsymbol{c}_{12}\end{bmatrix} \\ \boldsymbol{\Gamma}_{\boldsymbol{v},1} = \boldsymbol{\Gamma}_{\boldsymbol{v}} \end{cases}, \tag{8}$$

where $\boldsymbol{c}_i$ is the ith row vector of $\mathbf{C}_1$. For state q_2 representing GPS anomaly, the components $\left\{p_x, p_y\right\}$ of $\boldsymbol{x}$ may be incorrectly

Table 1
Multicopter model information.

Type	SCS-based model	SHS-based model
Plant	described in (5) and Fig. 3(a)	described in (7) and Fig. 3(b)
Controller	described in (2)&(3)	described in (2)&(3)
Observer	Extended Kalman Filter (EKF)	a modified IMM-based algorithm

measured, even the GPS measurements are completely lost. Then, we have

$$\mathbf{C}_2 = \mathbf{C}_1 \backslash \begin{bmatrix} \boldsymbol{c}_1 \\ \boldsymbol{c}_2 \end{bmatrix}, \tag{9}$$

which is interpreted that $\mathbf{C}_2$ is the rest part of subtracting the rows $\boldsymbol{c}_1$ and $\boldsymbol{c}_2$ from $\mathbf{C}_1$. The meaning of $\mathbf{C}_2$ is that when a GPS anomaly occurs, the continuous dynamics under state q_2 does not consider GPS measurements, despite whether the GPS can generate measurements or not. According to this principle, for states q_3 and q_4, we have

$$\begin{array}{l} \mathbf{C}_3 = \mathbf{C}_1 \backslash \boldsymbol{e}_3 \\ \mathbf{C}_4 = \mathbf{C}_1 \backslash \boldsymbol{e}_9 \end{array}, \tag{10}$$

because the height p_z and the yaw angle ψ are the 3rd and 9th components of $\boldsymbol{x}$, respectively. The observation noise $\boldsymbol{v}$ and the corresponding noise driven matrix $\boldsymbol{\Gamma}_{\boldsymbol{v}}$ under states q_2, q_3 and q_4 can be also obtained following the similar variation of the matrix $\mathbf{C}_j$.

It should be indicated that (7) determines the stochastic kernel $T_x(\cdot|\boldsymbol{s})$. Note that the stochastic kernel $T_x(\cdot|\boldsymbol{s})$ is different for different health statuses, because the forms of $\mathbf{C}_j$ and $\boldsymbol{\Gamma}_{\boldsymbol{v},j}\boldsymbol{v}_j$ are inconsistent for different health statuses. For the stochastic kernel $T_q(\cdot|\boldsymbol{s})$, it reflects the transitions among different health statuses. Here, the discrete dynamics is a first-order Markov chain with transition probabilities as

$$\mathcal{P}\left\{q_j(k+1)\,|q_i(k)\right\} = \pi_{ij}(k), \ \forall q_i, q_j \in \mathcal{Q},$$

and

$$\sum_{j=1}^{m} \pi_{ij}(k) = 1, \ i = 1, 2, \cdots, m.$$

The failure rate or anomaly rate of onboard components in a multicopter and the related reliability test data are helpful for determining the value of the transition probability π_{ij}. For the stochastic kernel $R\left(\cdot\left|\boldsymbol{s}, q'\right.\right)$, we can let $R\left(\cdot\left|\boldsymbol{s}, q'\right.\right) = T_x(\cdot|\boldsymbol{s})$. This indicates that during the time step when the discrete transition occurs, the system process variables keep evolving according to the continuous dynamics of the previous discrete state before the transition.

Up to now, two kinds of multicopter model are presented. Table 1 summarizes the model information presented in this section.

Remark 3. The sub-model of state q_1 in the SHS-based model is an SCS-based model. This indicates that the SHS-based model is a more general model, which fits the requirement of health evaluation.

Remark 4. The SHS-based model can be extended for considering more kinds of unhealthy situations. For example, other sensors such as gyroscope anomaly can be also modeled as a new health status following the principles above. For propulsion system anomaly, especially for actuator anomaly, the form of the nonlinear function $\boldsymbol{f}(\cdot)$ with a control effectiveness matrix and the noise item $\boldsymbol{\Gamma}_{\boldsymbol{w}}\boldsymbol{w}$ can be modified to generate new health statuses.

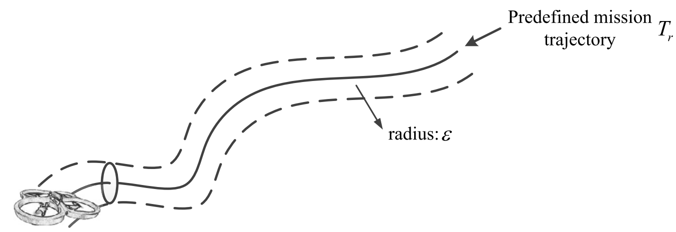

Fig. 4. Diagram of the predefined mission trajectory Tr and the tolerant threshold ε.

2.3. Health definition

In order to quantitatively evaluate the performance of the multicopter, a definition of the health degree is proposed for a multicopter. "Health" can be defined as an extent of system degradation or performance deviation from an expected normal condition [79]. A dynamical system is considered healthy if suitable for its intended purpose for an extended period of time and considered unhealthy if damaged or approaching a status of failure for its intended purpose [80]. In this case, an mathematical definition of health degree is proposed for a multicopter by referring to the safety assessment in SHS theory [40,41] and the real-time reliability evaluation in reliability theory [35–37].

A multicopter is always expected to execute a mission from the assignment of users. The mission can be described by a sequence of waypoints, indicating a mission trajectory. From a perspective of health of dynamical systems, a multicopter is considered healthy if it flies following the trajectory without deviation. Thus, the health degree is defined as a probability that the multicopter follows the mission trajectory. Suppose a multicopter has a predefined mission trajectory $Tr = \left\{\left(p_x^M, p_y^M, p_z^M\right), k\left|\left(p_x^M(k), p_y^M(k), p_z^M(k)\right) \in \mathbb{R}^3, \text{ for } k = 0, 1, 2, \cdots\right.\right\}$. Then, we propose definitions of instantaneous health degree and interval health degree.

Definition 2 *(Instantaneous health degree).* Given a mission trajectory Tr and the real position $\left(p_x(k), p_y(k), p_z(k)\right)$ of a multicopter at time k. Let

$$\Delta p(k) = \left\| \left(p_x(k), p_y(k), p_z(k)\right) - \left(p_x^M(k), p_y^M(k), p_z^M(k)\right) \right\|_2.$$

The instantaneous health degree at time k is defined as

$$H(k) = \mathcal{P}\left\{\Delta p(k) \leqslant \varepsilon \left| \forall q_j \in \mathcal{Q}\right.\right\}, \tag{11}$$

where $\varepsilon > 0$ represents the tolerant threshold of behavior deviation caused by anomalies as shown in Fig. 4.

Definition 3 *(Interval health degree).* Given a mission trajectory Tr and the real position $\left(p_x, p_y, p_z\right)$ of a multicopter over a time interval $[k_1, k_2]$. The interval health degree over a time interval $[k_1, k_2]$ is defined as

$$H(k_1, k_2) = \mathcal{P}\left\{\Delta p(j) \leqslant \varepsilon, \forall j \in [k_1, k_2] \left| \forall q_j \in \mathcal{Q}\right.\right\}. \tag{12}$$

Remark 5. As shown in Fig. 4, the envelope generated by the mission trajectory Tr and the tolerant threshold ε is called as a health set, which is similar as the safe set definition in the safety assessment research. For an assigned mission, its trajectory is predefined and known, and the tolerant threshold ε should be appropriately selected based on specific user requirements and engineering experience. On this basis, the instantaneous health degree is the probability that the multicopter remains within the health set at time k, no matter which discrete state it belongs to. It uses an instantaneous behavior of multicopter to measure its health, and the health degradation can be obtained immediately after the anomaly

Table 2
Procedure of the classic IMM algorithm.

1.	Interacting (for $j=1,2,\cdots,m$)
	1) predicted mode probability: $\mu_j(k\|k-1)\triangleq\mathcal{P}\left\{q_j(k)\|\mathbf{Y}^{k-1}\right\}=\sum_i\pi_{ij}\mu_i(k-1)$
	2) mixing probability: $\mu_{i\|j}(k-1)\triangleq\mathcal{P}\left\{q_i(k-1)\|q_j(k),\mathbf{Y}^{k-1}\right\}=\pi_{ij}\mu_i(k-1)/\mu_j(k\|k-1)$
	3) mixing estimate: $\hat{\boldsymbol{x}}_j^0(k-1\|k-1)\triangleq E\left[\boldsymbol{x}(k-1)\|q_j(k),\mathbf{Y}^{k-1}\right]=\sum_i\hat{\boldsymbol{x}}_i(k-1\|k-1)\mu_{i\|j}(k-1)$
	4) mixing covariance: $\mathbf{P}_j^0(k-1\|k-1)\triangleq\mathrm{cov}\left[\hat{\boldsymbol{x}}_j^0(k-1\|k-1)\left\|q_j(k),\mathbf{Y}^{k-1}\right.\right]=\sum_i\left[\mathbf{P}_i(k-1\|k-1)\right.$
	$\left.+\left[\hat{\boldsymbol{x}}_j^0(k-1\|k-1)-\hat{\boldsymbol{x}}_i(k-1\|k-1)\right]\left[\hat{\boldsymbol{x}}_j^0(k-1\|k-1)-\hat{\boldsymbol{x}}_i(k-1\|k-1)\right]^T\right]\mu_{i\|j}(k-1)$
2.	Model-conditional filtering (for $j=1,2,\cdots,m$)
	1) predicted state: $\hat{\boldsymbol{x}}_j(k\|k-1)\triangleq E\left[\boldsymbol{x}(k)\|q_j(k),\mathbf{Y}^{k-1}\right]=\boldsymbol{f}_j\left(\hat{\boldsymbol{x}}_j^0(k-1\|k-1),\boldsymbol{u}(k)\right)$
	2) predicted covariance: $\mathbf{P}_j(k\|k-1)\triangleq\mathrm{cov}\left[\hat{\boldsymbol{x}}_j(k\|k-1)\left\|q_j(k),\mathbf{Y}^{k-1}\right.\right]$
	$=\boldsymbol{A}_j(k-1)\mathbf{P}_j^0(k-1\|k-1)\boldsymbol{A}_j^T(k-1)+\boldsymbol{\Gamma}_{\boldsymbol{w},j}\mathbf{Q}_j\boldsymbol{\Gamma}_{\boldsymbol{w},j}^T$, where $\boldsymbol{A}_j(k-1)=\left.\frac{\partial\boldsymbol{f}_j}{\partial\boldsymbol{x}}\right\|_{\hat{\boldsymbol{x}}_j^0(k-1\|k-1),\boldsymbol{u}(k)}$
	3) measurement residual: $\boldsymbol{r}_j\triangleq\boldsymbol{y}(k)-E\left[\boldsymbol{y}(k)\|q_j(k),\mathbf{Y}^{k-1}\right]=\boldsymbol{y}(k)-\mathbf{C}_j(k)\hat{\boldsymbol{x}}_j(k\|k-1)$
	4) residual covariance: $\mathbf{S}_j\triangleq\mathrm{cov}\left[\boldsymbol{r}_j\left\|q_j(k),\mathbf{Y}^{k-1}\right.\right]=\mathbf{C}_j(k)\mathbf{P}_j(k\|k-1)\mathbf{C}_j^T(k)+\boldsymbol{\Gamma}_{\boldsymbol{v},j}\mathbf{R}_j\boldsymbol{\Gamma}_{\boldsymbol{v},j}^T$
	5) filter gain: $\mathbf{K}_j=\mathbf{P}_j(k\|k-1)\mathbf{C}_j^T(k)\mathbf{S}_j^{-1}$
	6) updated state: $\hat{\boldsymbol{x}}_j(k\|k)\triangleq E\left[\boldsymbol{x}(k)\|q_j(k),\mathbf{Y}^k\right]=\hat{\boldsymbol{x}}_j(k\|k-1)+\mathbf{K}_j\boldsymbol{r}_j$
	7) updated covariance: $\mathbf{P}_j(k\|k)\triangleq\mathrm{cov}\left[\hat{\boldsymbol{x}}_j(k\|k)\left\|q_j(k),\mathbf{Y}^k\right.\right]=\mathbf{P}_j(k\|k-1)-\mathbf{K}_j\mathbf{S}_j^T\mathbf{K}_j$
3.	Mode probability update (for $j=1,2,\cdots,m$)
	1) likelihood function: $\mathcal{L}_j(k)=\mathcal{N}\left(\boldsymbol{r}_j;\mathbf{0},\mathbf{S}_j\right)=\frac{1}{\sqrt{\|(2\pi)\mathbf{S}_j\|}}\exp\left(-\frac{1}{2}\boldsymbol{r}_j^T\mathbf{S}_j^{-1}\boldsymbol{r}_j\right)$
	2) mode probability: $\mu_j(k)\triangleq\mathcal{P}\left\{q_j(k)\|\mathbf{Y}^k\right\}=\frac{\mu_j(k\|k-1)\mathcal{L}_j(k)}{\sum_i\mu_i(k\|k-1)\mathcal{L}_i(k)}$
	3) mode estimation: $\mu_j(k)=\max_i\mu_i(k)\begin{cases}\geqslant\mu_T\Longrightarrow\text{The system is in mode } q_j\\ <\mu_T\Longrightarrow\text{No mode is recognized}\end{cases}$
4.	Estimate fusion (for the output purpose)
	1) overall estimate: $\hat{\boldsymbol{x}}(k\|k)\triangleq E\left[\boldsymbol{x}(k)\|\mathbf{Y}^k\right]=\sum_j\hat{\boldsymbol{x}}_j(k\|k)\mu_j(k)$
	2) overall covariance: $\mathbf{P}(k\|k)\triangleq E\left[\left[\boldsymbol{x}(k)-\hat{\boldsymbol{x}}(k\|k)\right]\left[\boldsymbol{x}(k)-\hat{\boldsymbol{x}}(k\|k)\right]^T\|\mathbf{Y}^k\right]$
	$=\sum_j\left[\mathbf{P}_j(k\|k)+\left[\hat{\boldsymbol{x}}(k\|k)-\hat{\boldsymbol{x}}_j(k\|k)\right]\left[\hat{\boldsymbol{x}}(k\|k)-\hat{\boldsymbol{x}}_j(k\|k)\right]^T\right]\mu_j(k)$
5.	$k=k+1$

occurs. Furthermore, the interval health degree is the probability that the multicopter remains within the health set over the time interval $[k_1,k_2]$, no matter which discrete state it belongs to. It focuses on a behavior over a time interval to evaluate system health, and it treats system health as a process indicator representing system features over a time interval. Both the definitions have their own advantages.

3. Health evaluation of multicopter

3.1. Problem formulation

For the presented SHS-based multicopter model $\mathcal{H}=\left(\mathcal{Q},n,Init,T_x,T_q,R\right)$, an initial distribution of the hybrid state $\boldsymbol{s}(0)=(q(0),\boldsymbol{x}(0))$ can be described as

$$\begin{cases}f\left(\boldsymbol{x}(0)\left|q_j(0)\right.\right)=\mathcal{N}\left(\hat{\boldsymbol{x}}_j(0),\mathbf{P}_j(0)\right)\\ \mathcal{P}\left\{q_j(0)\right\}=\mu_j(0)\end{cases},\ j=1,2,\cdots,m,$$

where $\mu_j(0)\geqslant 0$ for $\forall q_j\in\mathcal{Q}$, and $\sum_{j=1}^m\mu_j(0)=1$. Let $\mathbf{Y}^k=\{\boldsymbol{y}(0),\boldsymbol{y}(1),\cdots,\boldsymbol{y}(k)\}$ represent the sequence of sensor measurements up to time k. In order to calculate the health degree at time k by Definition 2, the distribution of the hybrid state $\boldsymbol{s}$ should be accurately estimated, including the pdf $f\left(\boldsymbol{x}(k)\left|q_j(k),\mathbf{Y}^k\right.\right)$ (*i.e.* distribution of process variables $\boldsymbol{x}(k)$ conditional on discrete state $q_j(k)$ and $\mathbf{Y}^k$) and the discrete state probability $\mathcal{P}\left(q(k)\left|\mathbf{Y}^k\right.\right)$. By the theorem of total probability, we have

$$f\left(\boldsymbol{x}(k)\left|\mathbf{Y}^k\right.\right)=\sum_{j=1}^m f\left(\boldsymbol{x}(k)\left|q_j(k),\mathbf{Y}^k\right.\right)\cdot\mathcal{P}_j\left(q_j(k)\left|\mathbf{Y}^k\right.\right). \tag{13}$$

Then, the health degree at time k is calculated as

$$H(k)=\int_\Omega f\left(\boldsymbol{x}(k)\left|\mathbf{Y}^k\right.\right)d\boldsymbol{x}, \tag{14}$$

where Ω is a polyhedron with a center $\left(p_x^M(k),p_y^M(k),p_z^M(k)\right)$ and a radius ε. For the health degree over a time interval $[k_1,k_2]$, assuming the time index conforms to uniform distribution for simplicity, we have

$$H(k_1,k_2)=\sum_{i=k_1}^{k_2}\frac{H(i)}{k_2-k_1}. \tag{15}$$

According to (13)–(15), the key of the health degree calculation is to accurately estimate the distribution of the hybrid state $\boldsymbol{s}$. In this case, an IMM-based algorithm [81] is employed here to achieve hybrid state estimation.

3.2. IMM-based health evaluation

3.2.1. Classic IMM algorithm

The classic IMM algorithm is a recursive estimator [81]. In each recursive cycle, it consists of four major steps: 1) model-conditional reinitialization (interacting or mixing of the estimates), where the input to the filter of each mode is obtained by mixing the estimates of all filters at the previous time under the assumption that the system is in this particular mode at the present time; 2) model-conditional filtering, performed in parallel for each mode; 3) mode probability update, based on the model-conditional likelihood functions; 4) estimate fusion, which yields the overall state estimate as the weighted sum of the updated state estimates of all filters. The procedure of the classic IMM algorithm is shown in Table 2. Note that the concept of mode in the IMM algorithm corresponds to the concept of discrete states in the SHS-based multicopter model.

Remark 6. For performing the classic IMM algorithm on the health evaluation of a multicopter with the SHS-based model, there are two deficiencies which are required to be modified. i) In the classic IMM algorithm, the transition probability is assumed to be constant over the studied time interval, and the transition probability from any particular anomaly mode to the normal mode is generally and artificially set larger than others in order to prevent a false fault diagnosis [82]. However, the unchanged transition probability can mislead the mode identification to intermittently declare a false alarm, especially when a fault-tolerant controller works well after the first anomaly occurs. This is because the model probability of the healthy mode tends to increase again as the current anomalous system converges to a steady state by the fault-tolerant control law after an anomaly occurs [83]. ii) Following the classic IMM algorithm, the real-time distribution of $f\left(\boldsymbol{x}(k)\left|q_j(k),\mathbf{Y}^k\right.\right)$ cannot be approximated as a Gaussian distribution, because the mixing covariance in *Step 1* will change the covariance of $\boldsymbol{x}$ under mode q_j in a non-Gaussian way. This will lead to a difficulty in the health degree calculation due to a non-Gaussian distribution of $f\left(\boldsymbol{x}(k)\left|q_j(k),\mathbf{Y}^k\right.\right)$.

In this case, two modifications are made to the classic IMM algorithm, and the health evaluation algorithm based on the modified IMM algorithm is proposed as follows.

3.2.2. Health evaluation based on the modified IMM algorithm

3.2.2.1. Modification 1 In current IMM research [81,82,84–86], the transition probability matrix is always assumed to be known and constant as prior knowledge. As indicated in Remark 6, the unchanged transition probability can mislead the mode identification to intermittently declare a false alarm. This problem can be solved by adjusting the transition probability matrix after an anomaly occurs. The principles are as follows.

i) Let the IMM "thinks" the normal (healthy) mode before the first anomaly occurrence is not the normal mode any more. The declared anomaly mode should be viewed as a new "normal" mode [83]. It means that if the model probability of a certain anomaly mode remains larger than that of any other mode for a specific time instance, the transition probability related to the corresponding anomaly mode should be increased. On the other hand, the transition probability related to the previous mode should be decreased to reflect the fact that the anomaly mode selected by the mode identification algorithm becomes currently dominant.

ii) The update process should be efficiently implemented, because most algorithms of transition probability estimation are with high computational complexity [82,87].

In this case, an update of transition probability is added to the classic IMM algorithm. Suppose the system is in mode q_i at time $k-1$, and in mode q_j at time k, $q_i \neq q_j$. Let $\Pi(k)=\left[\pi_{ij}(k)\right]_{m\times m}$ be the transition probability matrix. Further define an elementary matrix as

$$\Theta=\begin{bmatrix} 1 & & & & & \\ & \cdots & & & & \\ & & 0 & & 1 & \leftarrow i\text{th row} \\ & & & \ddots & & \\ & & 1 & & 0 & \leftarrow j\text{th row} \\ & & & & & \cdots \\ & & & & & & 1 \end{bmatrix}_{m\times m}. \tag{16}$$

Then, the transition probability matrix $\mathbf{\Pi}(k)$ is updated as

$$\mathbf{\Pi}(k)=\Theta\cdot\mathbf{\Pi}(k-1)\cdot\Theta,$$

which means $\mathbf{\Pi}(k)$ is obtained from $\mathbf{\Pi}(k-1)$ by an elementary row transformation and an elementary column transformation. After the update, mode q_j at time k becomes currently dominant instead of mode q_i. In Section 4, this modification is validated to be a necessary step, and a guarantee for correct mode identification. This is because the restriction that real discrete dynamics should be precisely known as *a priori* is relaxed.

3.2.2.2. Modification 2 As indicated in Remark 6, the real-time distribution of $f\left(\boldsymbol{x}(k)\left|q_j(k),\mathbf{Y}^k\right.\right)$ cannot be approximated as a Gaussian distribution following the classic IMM algorithm. In this case, a modification is performed on the IMM algorithm by let $\mathbf{P}_j^0(k-1|k-1)=\mathbf{P}_j(k-1|k-1)$ in Table 2. Actually, without the covariance mixing process, it will not degrade the performance of the IMM algorithm in our research, which will be shown in Section 4. Thus, the pdf $f\left(\boldsymbol{x}(k)\left|q_j(k),\mathbf{Y}^k\right.\right)$ can be approximated as [88,89]

$$f\left(\boldsymbol{x}(k)\left|q_j(k),\mathbf{Y}^k\right.\right)=\mathcal{N}\left(\hat{\boldsymbol{x}}_j(k|k),\mathbf{P}_j(k|k)\right).$$

By applying *Modifications 1&2* to the classic IMM algorithm, the health evaluation is performed on the SHS-based multicopter model based on the modified IMM algorithm. The diagram of the health evaluation process is shown in Fig. 5, and the details of the algorithm are presented in Table 3.

4. A case study: multicopter with sensor anomalies

In this section, the proposed health evaluation method is performed on a multicopter with sensor anomalies. The sensors GPS, barometer and compass are considered alternately unhealthy in the simulation. The SHS-based model configuration, simulated flight data generation and health evaluation results are presented. Also, discussions and some comparisons are given in this section.

4.1. Model configuration

The parameters in the SHS-based model presented in Section 2 are listed in Table 4.

Remark 7. For ease of visualization, the controllers of different health statuses are identical, which will make readers easy to view the performance deviation from the expected normal condition. Actually, for the purpose of safety decision-making, the controller of different health statuses should be set to be different. For example, when the GPS anomaly is detected, the controller should be changed to perform returning home or landing rather than continue to execute the predetermined mission.

For the system noise $\boldsymbol{w}$ and the noise driven matrix $\mathbf{\Gamma}_{\boldsymbol{w}}$, set

$$\begin{aligned}&\boldsymbol{w}(\cdot)\sim\mathcal{N}(\mathbf{0},\mathbf{Q})\\&\mathbf{\Gamma}_{\boldsymbol{w}}=\mathrm{diag}\{0,0,0,1,1,1,0,0,0,1,1,1\}\end{aligned}$$

where

$$\begin{aligned}\mathbf{Q}=\mathrm{diag}\{&0.01,0.01,0.01,0.01,0.01,0.01,0.001,0.001,0.001,\\&0.001,0.001,0.001\}.\end{aligned}$$

For measurement noise $\boldsymbol{v}_j$ and noise driven matrix $\mathbf{\Gamma}_{\boldsymbol{v},j}$ under each state q_j, set

$$q_1:\begin{cases}\boldsymbol{v}_1(\cdot)\sim\mathcal{N}(\mathbf{0},\mathbf{R}_1)\\ \mathbf{R}_1=\mathrm{diag}\{0.2,0.2,0.2,0.5,0.5,0.5,0.001,0.001,\\ \qquad 0.001,0.001,0.001,0.001\}\\ \mathbf{\Gamma}_{\boldsymbol{v},1}=\mathrm{diag}\{1,1,1,1,1,1,1,1,1,1,1,1\}\end{cases}.$$

For states q_2, q_3 and q_4, the matrices $\mathbf{R}_j$ and $\mathbf{\Gamma}_{\boldsymbol{v},j}$ can be obtained following the principles as presented in (8)–(10). Referring to [81,82,84,85], the transition probability matrix representing discrete dynamics is set as

$$\mathbf{\Pi}=\begin{bmatrix}0.97&0.01&0.01&0.01\\0.1&0.9&0&0\\0.1&0&0.9&0\\0.1&0&0&0.9\end{bmatrix}.$$

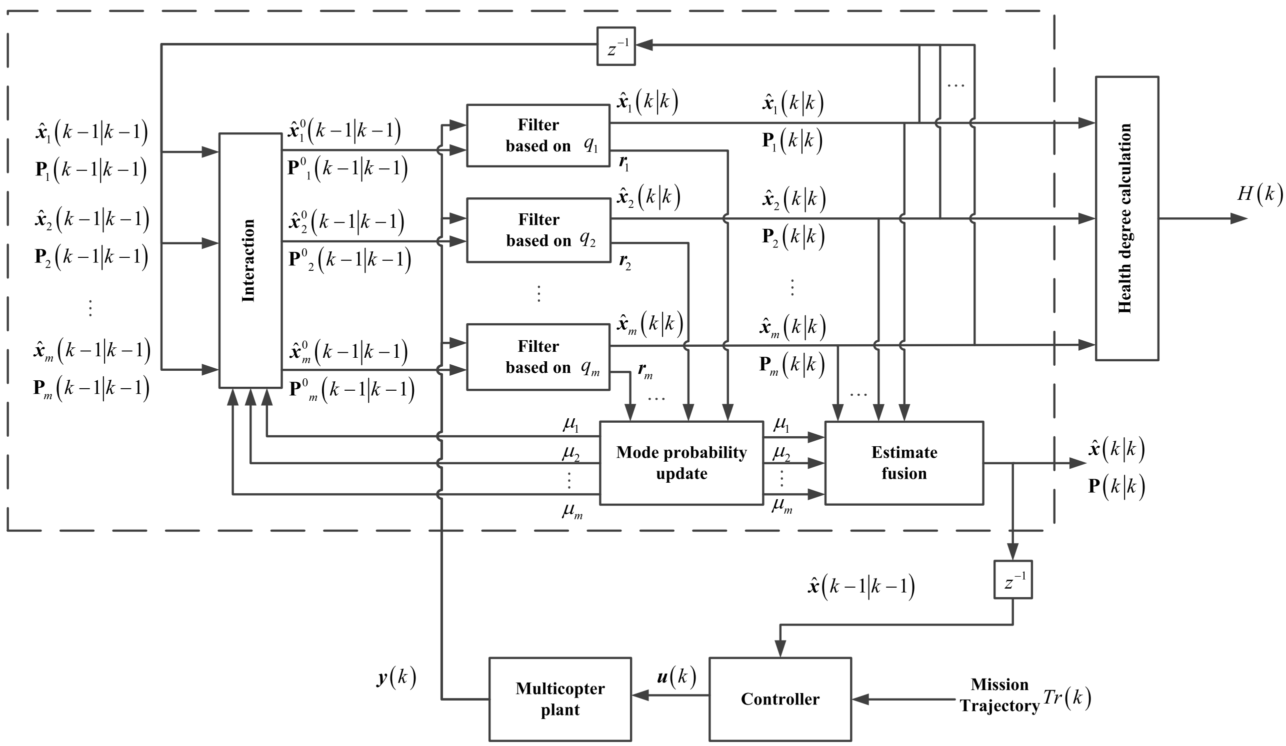

Fig. 5. Diagram of IMM-based health evaluation algorithm. This diagram is a comprehensive format of Fig. 1 by employing the SHS-based multicopter model and the IMM-based health evaluation algorithm.

Table 3
Procedure of the health evaluation algorithm.

1.	Interacting (for $j = 1, 2, \cdots, m$)
	1) predicted mode probability: $\mu_j(k|k-1) \triangleq \mathcal{P}\{q_j(k)|\mathbf{Y}^{k-1}\} = \sum_i \pi_{ij}(k-1)\mu_i(k-1)$
	2) mixing probability: $\mu_{i|j}(k-1) \triangleq \mathcal{P}\{q_i(k-1)|q_j(k), \mathbf{Y}^{k-1}\} = \pi_{ij}(k-1)\mu_i(k-1)/\mu_j(k|k-1)$
	3) mixing estimate: $\hat{\boldsymbol{x}}_j^0(k-1|k-1) \triangleq E[\boldsymbol{x}(k-1)|q_j(k), \mathbf{Y}^{k-1}] = \sum_i \hat{\boldsymbol{x}}_i(k-1|k-1)\mu_{i|j}(k-1)$
	4) setting covariance: $\mathbf{P}_j^0(k-1|k-1) = \mathbf{P}_j^0(k-1|k-1)$
2.	Model-conditional filtering (for $j = 1, 2, \cdots, m$)
	1) same with 1)–7) presented in Table 2
3.	Mode probability update (for $j = 1, 2, \cdots, m$)
	1) same with 1)–7) presented in Table 2
4.	Estimate fusion (for the output purpose)
	1) overall estimate: $\hat{\boldsymbol{x}}(k|k) \triangleq E[\boldsymbol{x}(k)|\mathbf{Y}^k] = \sum_j \hat{\boldsymbol{x}}_j(k|k)\mu_j(k)$
5.	Update transition probability matrix
	1) set elementary matrix Θ: Given $q_i = q(k-1), q_j = q(k)$, set Θ by (16)
	2) update: $\mathbf{\Pi}(k) = \Theta \cdot \mathbf{\Pi}(k-1) \cdot \Theta$
6.	Health degree calculation
	1) calculate the instantaneous health degree and interval health degree by (13), (14) and (15)
7.	$k = k+1$

Table 4
Multicopter model parameters.

m	1.535 kg
J_x, J_y, J_z	$0.0411, 0.0478, 0.0599$ kg·m^2
g	9.8 m/s^2
T	0.01 s
$k_{P,z}, k_{D,z}$	10, 8
$k_{P,\phi}, k_{D,\phi}$	5, 0.8
$k_{P,\theta}, k_{D,\theta}$	5, 0.8
$k_{P,\psi}, k_{D,\psi}$	5, 0.4
$\mathbf{K}_{Pa}, \mathbf{K}_{Da}$	$\mathbf{I}_2, 2\mathbf{I}_2$

It can be seen that the state q_1 is dominant in the configuration of $\mathbf{\Pi}$. However, the transition probability matrix will be updated in the modified IMM algorithm. Thus, the restriction that real discrete dynamics should be precisely known as *a priori* is relaxed.

4.2. Simulated flight data generation

Here, equation (7) is used to generate real flight data under different anomalies, including true values of process variables of the multicopter and their measurements. In the simulation, different anomalies occur alternately as shown in Table 5. The whole simulation time is 160 s, and the sample time $T = 0.01$ s.

The observation equation of (7) is used to generate system measurements under the fully healthy status. For simulating GPS measurement with big noise, the related parameters of covariance matrix $\mathbf{R}_1$ of $\boldsymbol{v}_1(\cdot)$ is temporally increased as

$$\mathbf{R}_1(1,1) = \mathbf{R}_1(2,2) = 2.2.$$

For GPS measurement drift, add a random value to the measurements p_x and p_y as shown below

Table 5
Simulated flight data generation.

Time interval Anomaly type	0–6 s fully healthy	6 s–20 s GPS measurement with big noise	20 s–30 s fully healthy
Time interval Anomaly type	30 s–40 s barometer measurement with big noise	40 s–50 s compass measurement with big noise	50 s–60 s GPS measurement drift
Time interval Anomaly type	60 s–70 s fully healthy	70 s–90 s barometer measurement drift	90 s–100 s fully healthy
Time interval Anomaly type	100 s–130 s barometer measurement lost	130 s–160 s GPS measurement lost	

$$\begin{cases} \boldsymbol{y}(k) = \mathbf{C}_1 \boldsymbol{x}(k-1) + \boldsymbol{\Gamma}_{\boldsymbol{v},1} \boldsymbol{v}_1(k) + \Delta_p(k) \\ \Delta_p(k) = \left[\Delta p_x(k), \Delta p_y(k), 0, \cdots, 0\right]^T \\ \Delta p_x(k) = 1 + \xi_x(k) \\ \Delta p_y(k) = 2 + \xi_y(k) \\ \xi_x(\cdot) \sim \mathcal{N}(0, 0.1), \xi_y(\cdot) \sim \mathcal{N}(0, 0.1) \end{cases}.$$

For loss of GPS measurements, (7) is changed to

$$\begin{cases} y_1(k) = y_1(k-1) \\ y_2(k) = y_2(k-1) \end{cases}.$$

For barometer and compass anomalies, similar process is performed to generate related measurements.

4.3. Health evaluation results

The proposed health evaluation algorithm is performed on the SHS-based multicopter with the generated flight data in Table 5. The results are shown in Figs. 6–11. According to Definitions 2 and 3, the components $\{p_x, p_y, p_z\}$ in $\boldsymbol{x}$ are most concerned in the health evaluation of multicopters. Fig. 6 shows the variation of measurements and the estimated values of $\{p_x, p_y, p_z\}$. Fig. 7 depicts true values, expected values and estimated values with 95% confidence interval of $\{p_x, p_y, p_z\}$. Fig. 8 compares the estimation results by using the SHS-based model and the SCS-based model. From Figs. 6–8, it can be concluded that: 1) despite the incorrect system measurements, even measurements lost, the process variables $\boldsymbol{x}$ can be also estimated. 2) When sensor anomaly (especially measurements lost) occurs, the estimated values will deviate from the true values for related components in $\boldsymbol{x}$. 3) The estimated values are close to the expected values, because the controller of the multicopter always "thinks" that it makes the multicopter fly along the expected trajectory, despite the true trajectory deviates. 4) By using the modified IMM algorithm, both the estimate values of $\boldsymbol{x}$ and the covariance matrix are obtained. Thus, a 95% confidence interval is displayed in Fig. 7, which covers the true trajectory of the multicopter. Note that when the estimate values of $\boldsymbol{x}$ are precise, the confidence interval is narrow, which cannot be clearly depicted. 5) Compared with the estimation results with the SCS-based model, system variables can be estimated with smaller errors in a short time horizon with the SHS-based model after anomaly happens. It means that the SHS-based model is better and more robust than a single dynamic model for the purpose of health evaluation.

Figs. 9 and 10 present the probabilities of different health statuses and state identification results based on the modified IMM algorithm, and the performance is compared with the classic IMM algorithm. The result shows that by updating the transition probability matrix, the modified IMM algorithm performs better than the classic one. After obtaining the pdf $f\left(\boldsymbol{x}(k) \left| q_j(k), \mathbf{Y}^k\right.\right)$ and the probability $\mathcal{P}\left(q(k) \left| \mathbf{Y}^k\right.\right)$ of (13) as shown in Figs. 7 and 9, the health degree can be calculated according to (14) and (15). Here, the tolerant threshold ε in Definitions 2 and 3 is set to 0.3 m. The instantaneous health degree is calculated for each sample time T, and the interval health degree is calculated for every 5 seconds interval. The result is shown in Fig. 11. From Fig. 11, it can be seen that the health degree will decrease when sensor anomalies occurs, which proves the variation of health degree is able to reflect system anomalies and performance degradation. Here, two comparative health evaluation results are also presented. 1) As shown in Fig. 8, the distribution of process variables can be also obtained by EKF based on the SCS-based model. On this basis, the health degree is calculated and depicted in Fig. 12. Comparing Fig. 11 with Fig. 12, it indicates that the health degree calculated by the modified IMM algorithm and the SHS-based model is more accurate than that calculated by EKF and the SCS-based model. This is because the distribution of process variables estimated by the modified IMM algorithm is more accurate than that estimated by EKF, which has been shown in Fig. 8. 2) Fig. 6 shows the estimate of $\{p_x, p_y, p_z\}$. Existed research usually gets the health information of a dynamical system by comparing the estimated value of process variables with a health set. If the values of process variables at a time index or over a time interval are in the range of the health set, the system is considered healthy (the health degree is 1); otherwise, the system is considered unhealthy (the health degree is 0). Following this principle, the estimated values of $\{p_x, p_y, p_z\}$ are compared to the health set, and the result is shown in Fig. 13. Comparing Fig. 11 with Fig. 13, it reflects that the health degree is more sensitive to anomalies than the health evaluation result merely obtained by a comparison between system process variables and the health set. This is because the definition of health degree introduces the probability measure to health eval-

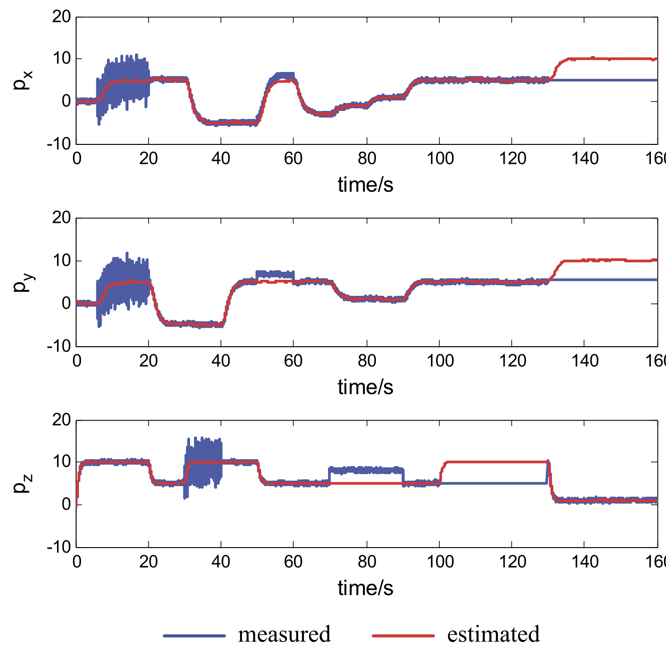

Fig. 6. Measurements and estimates of $\{p_x, p_y, p_z\}$.

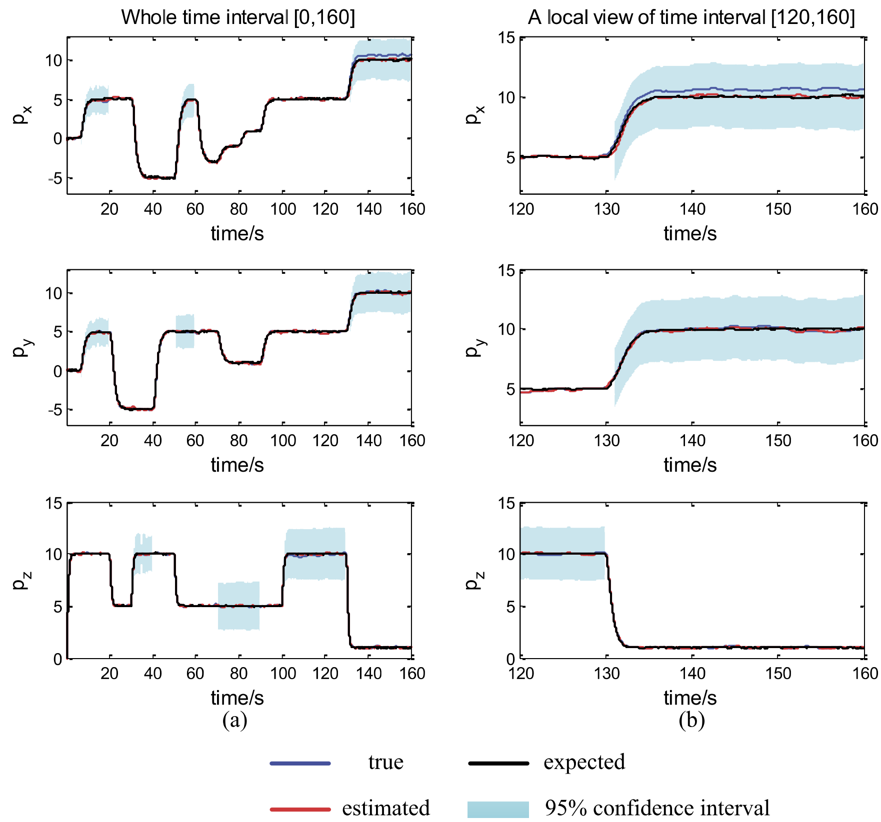

Fig. 7. True values, expected values, and estimates with 95% confidence interval of $\{p_x, p_y, p_z\}$. (For interpretation of the colors in this figure, the reader is referred to the web version of this article.)

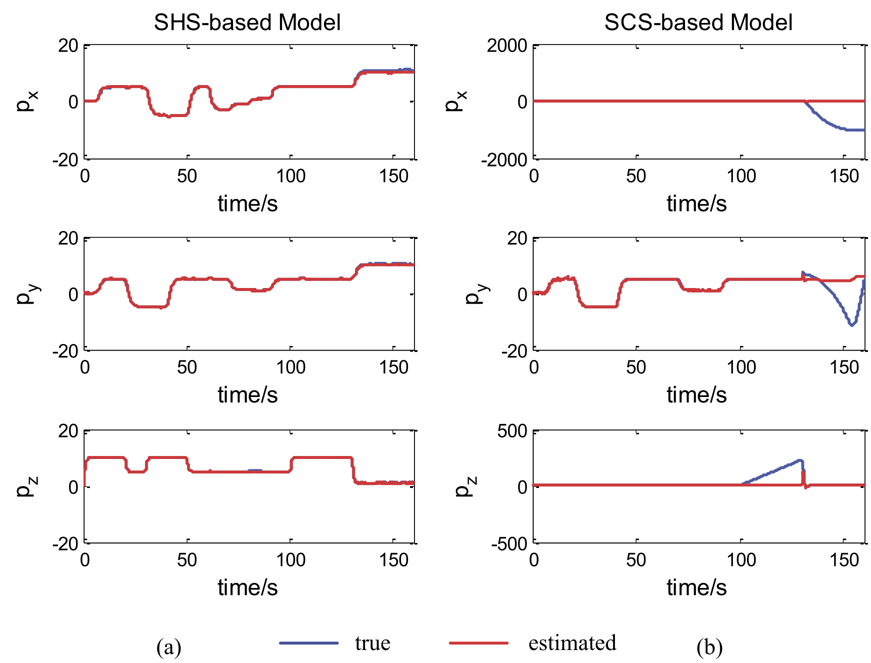

Fig. 8. Process variable estimation based on the SHS-based model and the SCS-based model.

uation by considering uncertainties, which is more appropriate for health evaluation of dynamical systems. As to the practical application of the proposed method, since the IMM-based algorithm is based on filtering techniques, it is easy to implement the whole algorithm in practical engineering. As to the instantaneity, the presented case study is simulated by MATLAB R2010b on a desktop. The average operating time of each cycle is less than 1 ms, meaning that compared to the sample time $T = 0.01$ s, the proposed health evaluation method is able to satisfy the instantaneity requirement.

5. Conclusion

This paper proposes a health evaluation method of multicopters. The multicopter is modeled by SHS, and its health is quantitatively measured by introducing a definition of health de-

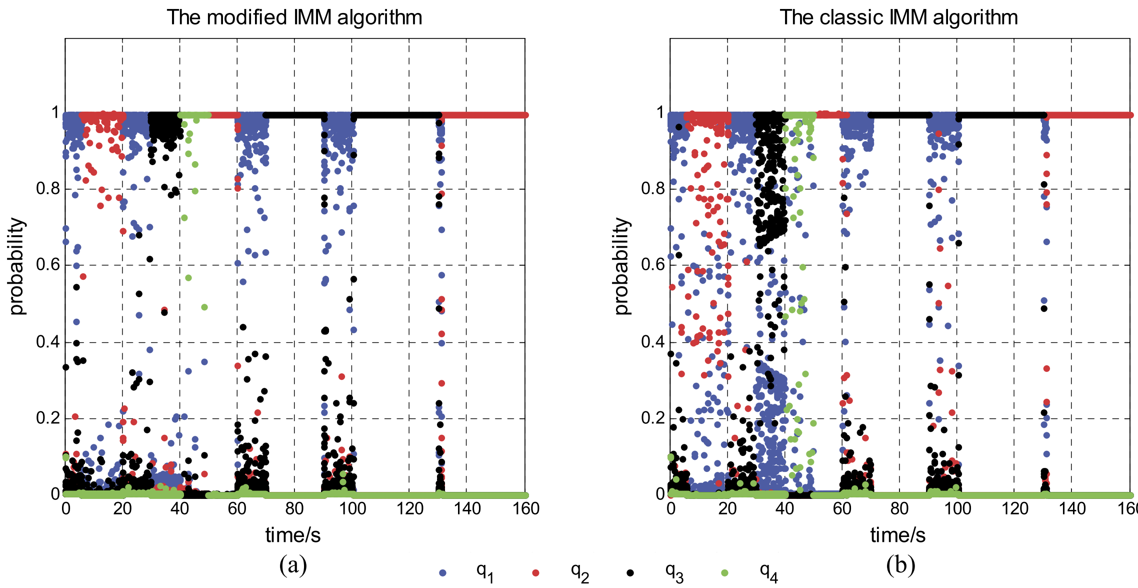

Fig. 9. Health status probability obtained by the modified IMM algorithm and the classic IMM algorithm. (For interpretation of the colors in this figure, the reader is referred to the web version of this article.)

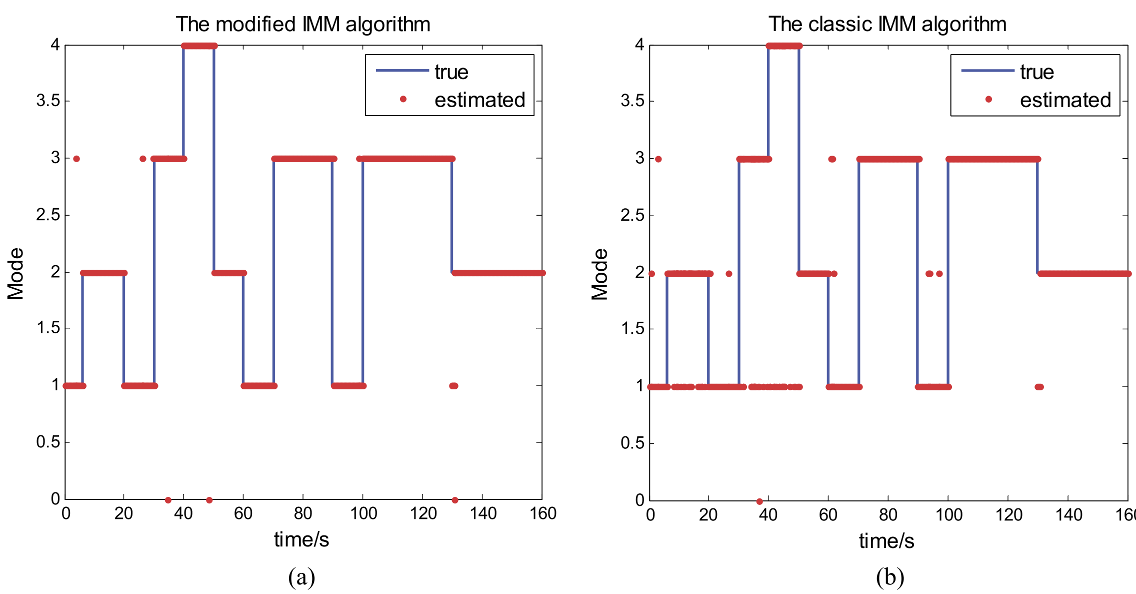

Fig. 10. Health status identification result obtained by the modified IMM algorithm and the classic IMM algorithm.

gree. Then, a modified IMM algorithm is proposed to estimate real-time hybrid state distribution. On this basis, the health degree is calculated. A case study of multicopter with sensor anomalies is presented to validate the effectiveness of the proposed method. The advantages of the SHS-based multicopter modeling and the health evaluation method presented in this paper are summarized in three aspects: 1) the SHS-based modeling concerns the safety issue of multicopters. The discrete and continuous dynamics in SHS can model different health statuses and corresponding dynamic behaviors. The simulation results show that the performance of the SHS-based model behaves better than the SCS-based model. 2) The health degree introduced in this paper gives a quantitative indicator of system performance, which is beneficial to pilots for understanding the working condition of multicopters. 3) The modified IMM algorithm outputs the multivariate Gaussian distribution of system process variables rather than just the estimated values, which provides more useful information about multicopter performance, especially when anomaly occurs. In future research, the proposed method can be extended in three aspects: 1) other anomalies such as propulsion system anomaly and communication breakdown can be added into the SHS-based multicopter model to extend the applicability of the proposed method. 2) Since the health degree is calculated on the system process variables, the health evaluation result is sensitive to external disturbances, which bring fluctuations to process variables. In order to solve this problem, the wind model should be added in the SHS-based multicopter model, or a health evaluation algorithm of a homogeneous multicopter team should be established. The two manners can effectively evaluate the amplitude and form of the external disturbance, and eliminate its influence on health degree calculation. 3) After health evaluation, health prediction and management is the next procedures of the PHM system as shown in Fig. 1. The concept of stochastic reachability has been already presented to predict system behavior in SHS research [41,90]. Combining the health prediction and stochastic reachability to extend the current work is an emphasis of future research. As to the management

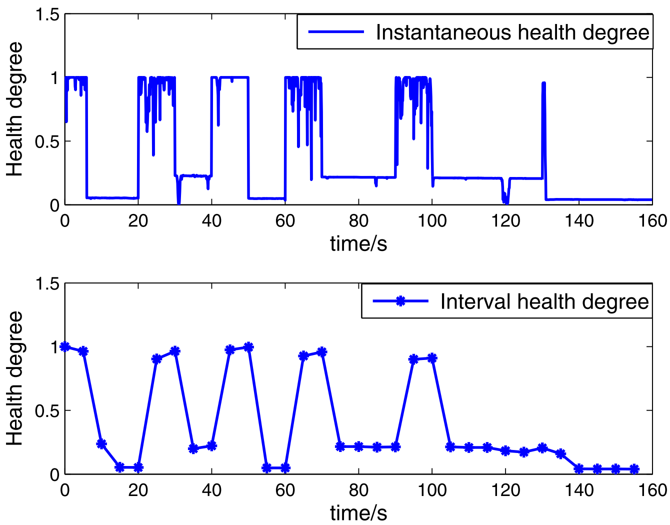

Fig. 11. Health degree calculated by the modified IMM algorithm based on the SHS-based model.

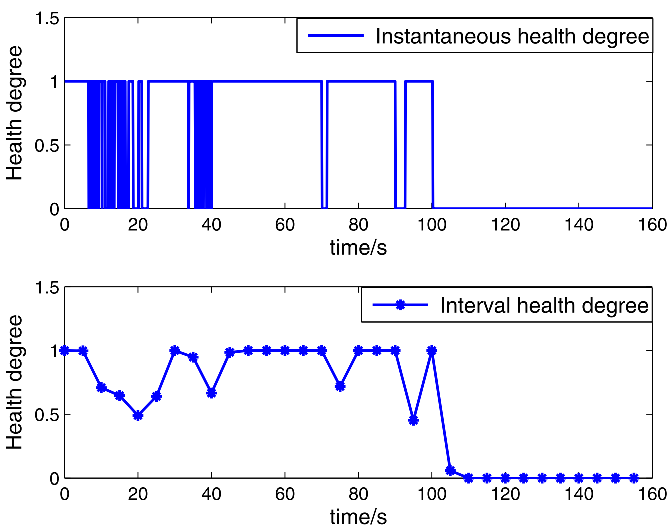

Fig. 12. Health degree calculated by EKF based on the SCS-based model.

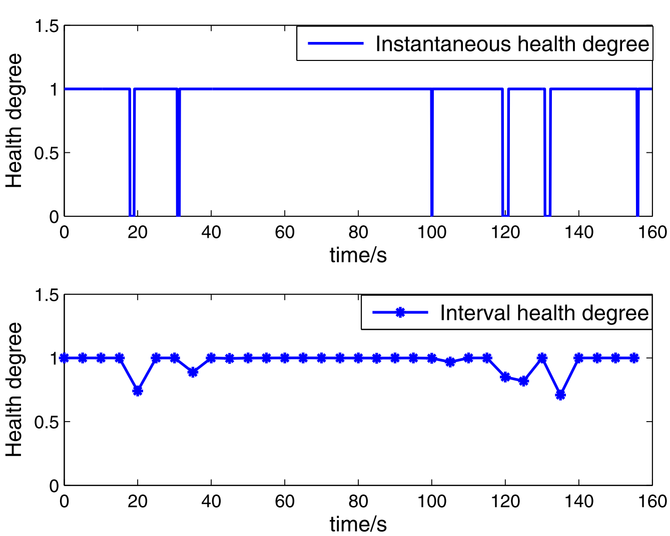

Fig. 13. Health evaluation calculated by a comparison between system process variables and the health set.

level, a multicopter failsafe mechanism dealt with multiple failures will be also established based on health evaluation results in future research.

Conflict of interest statement

There is no conflict of interest.

References

[1] T. Tomic, K. Schmid, P. Lutz, et al., Toward a fully autonomous UAV: research platform for indoor and outdoor urban search and rescue, IEEE Robot. Autom. Mag. 19 (3) (2012) 46–56.
[2] M.A. Goodrich, B.S. Morse, D. Gerhardt, et al., Supporting wilderness search and rescue using a camera-equipped mini UAV, J. Field Robot. 25 (1–2) (2008) 89–110.
[3] A. Agha-mohammadi, N.K. Ure, J.P. How, et al., Health aware stochastic planning for persistent package delivery missions using quadrotors, in: 2014 IEEE/RSJ International Conference on Intelligent Robots and Systems, IEEE, 2014, pp. 3389–3396.
[4] A.R. Girard, A.S. Howell, J.K. Hedrick, Border patrol and surveillance missions using multiple unmanned air vehicles, in: Decision and Control, 2004. 43rd IEEE Conference on CDC, vol. 1, IEEE, 2004, pp. 620–625.
[5] B. Bethke, J.P. How, J. Vian, Multi-UAV persistent surveillance with communication constraints and health management, in: AIAA Guidance, Navigation, and Control Conference (GNC), 2009.
[6] P. Chamoso, W. Raveane, V. Parra, et al., UAVs applied to the counting and monitoring of animals, in: Ambient Intelligence-Software and Applications, Springer International Publishing, 2014, pp. 71–80.
[7] Y. Huang, W.C. Hoffman, Y. Lan, et al., Development of a low-volume sprayer for an unmanned helicopter, J. Agric. Sci. 7 (1) (2015) 148–153.
[8] K.P. Valavanis, G.J. Vachtsevanos, Handbook of Unmanned Aerial Vehicles, Springer Publishing Company, Incorporated, 2014.
[9] M. Pecht, R. Jaai, A prognostics and health management roadmap for information and electronics-rich systems, Microelectron. Reliab. 50 (3) (2010) 317–323.
[10] D. Dimogianopoulos, J. Hios, S. Fassois, Aircraft engine health management via stochastic modelling of flight data interrelations, Aerosp. Sci. Technol. 16 (1) (2012) 70–81.
[11] D. Simon, A comparison of filtering approaches for aircraft engine health estimation, Aerosp. Sci. Technol. 12 (4) (2008) 276–284.
[12] G. Aaseng, A. Patterson-Hine, C. Garcia-Galan, A review of system health state determination methods, in: 1st Space Exploration Conference, Orlando, FL, 2005.
[13] A. Arnaiz, S. Ferreiro, M. Buderath, New decision support system based on operational risk assessment to improve aircraft operability, Proc. Inst. Mech. Eng. Part O, J. Risk Reliab. 224 (3) (2010) 137–147.
[14] N.K. Ure, G. Chowdhary, J.P. How, et al., Health aware planning under uncertainty for uav missions with heterogeneous teams, in: European Control Conference (ECC), Switzerland, 2013, pp. 3312–3319.
[15] A. Freddi, S. Longhi, A. Monteriu, A model-based fault diagnosis system for a mini-quadrotor, in: Proc. 2009 7th Workshop on Advanced Control and Diagnosis, 2009, pp. 19–20.
[16] A. Freddi, S. Longhi, A. Monteriu, M. Prist, Actuator fault detection and isolation system for an hexacopter, in: 2014 IEEE/ASME 10th International Conference on Mechatronic and Embedded Systems and Applications (MESA), IEEE, 2014, pp. 1–6.
[17] M. Frangenberg, J. Stephan, W. Fichter, Fast actuator fault detection and reconfiguration for multicopters, in: AIAA Guidance, Navigation and Control Conference, 2015, p. 1766.
[18] N. Meskin, K. Khorasani, C.A. Rabbath, A hybrid fault detection and isolation strategy for a network of unmanned vehicles in presence of large environmental disturbances, IEEE Trans. Control Syst. Technol. 18 (6) (2010) 1422–1429.
[19] M. Saied, H. Shraim, C. Francis, I. Fantoni, B. Lussier, Actuator fault diagnosis in an octorotor UAV using sliding modes technique: theory and experimentation, in: Control Conference (ECC), 2015 European, IEEE, 2015, pp. 1639–1644.
[20] M. Blanke, M. Staroswiecki, N.E. Wu, Concepts and methods in fault-tolerant control, in: American Control Conference, 2001. Proceedings of the 2001, Vol. 4, IEEE, 2001, pp. 2606–2620.
[21] G.P. Falconi, F. Holzapfel, Adaptive fault tolerant control allocation for a hexacopter system, in: American Control Conference (ACC), 2016, American Automatic Control Council (AACC), 2016, pp. 6760–6766.
[22] Z.T. Dydek, A.M. Annaswamy, E. Lavretsky, Adaptive control of quadrotor UAVs: a design trade study with flight evaluations, IEEE Trans. Control Syst. Technol. 21 (4) (2013) 1400–1406.
[23] Y. Zhang, J. Jiang, Integrated design of reconfigurable fault-tolerant control systems, J. Guid. Control Dyn. 24 (1) (2001) 133–136.
[24] C.T. Raabe, S. Suzuki, Adaptive failure-tolerant control for hexacopters, in: AIAA Infotech@ Aerospace Conference, in: Guidance, Navigation, and Control and Co-Located Conferences, American Institute of Aeronautics and Astronautics, 2013.

[25] C. Gao, G. Duan, Fault diagnosis and fault tolerant control for nonlinear satellite attitude control systems, Aerosp. Sci. Technol. 33 (1) (2014) 9–15.
[26] J.W. Sheppard, M. Kaufman, T.J. Wilmer, IEEE standards for prognostics and health management, IEEE Aerosp. Electron. Syst. Mag. 24 (9) (2009) 34–41.
[27] V. Venkatasubramanian, R. Rengaswamy, K. Yin, S.N. Kavuri, A review of process fault detection and diagnosis: Part I: Quantitative model-based methods, Comput. Chem. Eng. 27 (3) (2003) 293–311.
[28] Z. Gao, C. Cecati, S.X. Ding, A survey of fault diagnosis and fault-tolerant techniques—Part I: fault diagnosis with model-based and signal-based approaches, IEEE Trans. Ind. Electron. 62 (6) (2015) 3757–3767.
[29] G. Wang, Z. Huang, Data-driven fault-tolerant control design for wind turbines with robust residual generator, IET Control Theory Appl. 9 (7) (2015) 1173–1179.
[30] Z. Sun, S.J. Qin, A. Singhal, L. Megan, Control performance monitoring via model residual assessment, in: American Control Conference (ACC), 2012, June, IEEE, 2012, pp. 2800–2805.
[31] G. Bai, P. Wang, C. Hu, A self-cognizant dynamic system approach for prognostics and health management, J. Power Sources 278 (2015) 163–174.
[32] E. Zio, F. Di Maio, A data-driven fuzzy approach for predicting the remaining useful life in dynamic failure scenarios of a nuclear system, Reliab. Eng. Syst. Saf. 95 (1) (2010) 49–57.
[33] Z. Feng, M. Liang, F. Chu, Recent advances in time-frequency analysis methods for machinery fault diagnosis: a review with application examples, Mech. Syst. Signal Process. 38 (1) (2013) 165–205.
[34] P. Henriquez, J.B. Alonso, M. Ferrer, C.M. Travieso, Review of automatic fault diagnosis systems using audio and vibration signals, IEEE Trans. Syst. Man Cybern. 44 (5) (2014) 642–652.
[35] H. Lu, W.J. Kolarik, H. Lu, Real-time performance reliability prediction, IEEE Trans. Reliab. 50 (4) (2001) 353–357.
[36] K. Cai, Introduction to Fuzzy Reliability, Kluwer Academic Publishers, New York, NY, USA, 1996.
[37] Z. Xu, Y. Ji, D. Zhou, A new real-time reliability prediction method for dynamic systems based on on-line fault prediction, IEEE Trans. Reliab. 58 (3) (2009) 523–538.
[38] Z. Zhao, Q. Quan, K.Y. Cai, A profust reliability based approach to prognostics and health management, IEEE Trans. Reliab. 63 (1) (2014) 26–41.
[39] X.D. Koutsoukos, D. Riley, Computational methods for verification of stochastic hybrid systems, IEEE Trans. Syst. Man Cybern., Part A, Syst. Hum. 38 (2) (2008) 385–396.
[40] A. Abate, J.P. Katoen, J. Lygeros, M. Prandini, Approximate model checking of stochastic hybrid systems, Eur. J. Control 16 (6) (2010) 624–641.
[41] A. Abate, M. Prandini, J. Lygeros, S. Sastry, Probabilistic reachability and safety for controlled discrete time stochastic hybrid systems, Automatica 44 (11) (2008) 2724–2734.
[42] W. Liu, I. Hwang, A stochastic approximation based state estimation algorithm for stochastic hybrid systems, in: American Control Conference (ACC), 2012, June, IEEE, 2012, pp. 312–317.
[43] W. Liu, I. Hwang, On hybrid state estimation for stochastic hybrid systems, IEEE Trans. Autom. Control 59 (10) (2014) 2615–2628.
[44] F.L. Discalea, H. Matt, I. Bartoli, et al., Health monitoring of UAV wing skin-to-spar joints using guided waves and macro fiber composite transducers, J. Intell. Mater. Syst. Struct. 18 (4) (2007) 373–388.
[45] J.A. Oliver, J.B. Kosmatka, C.R. Farrar, et al., Development of a composite UAV wing test-bed for structural health monitoring research, in: The 14th International Symposium on: Smart Structures and Materials & Nondestructive Evaluation and Health Monitoring, International Society for Optics and Photonics, 2007.
[46] Y. Jiang, Z. Zhiyao, L. Haoxiang, et al., Fault detection and identification for quadrotor based on airframe vibration signals: a data-driven method, in: Control Conference (CCC), 2015 34th Chinese, IEEE, 2015, pp. 6356–6361.
[47] I. Kressel, A. Handelman, Y. Botsev, et al., Evaluation of flight data from an airworthy structural health monitoring system integrally embedded in an unmanned air vehicle, in: 6th European Workshop on Structural Health Monitoring, 2012, pp. 193–200.
[48] I. Kressel, J. Balter, N. Mashiach, et al., High speed, in-flight structural health monitoring system for medium altitude long endurance unmanned air vehicle, in: EWSHM—7th European Workshop on Structural Health Monitoring, 2014.
[49] Z. Cen, H. Noura, Y. Al Younes, Robust fault estimation on a real quadrotor UAV using optimized adaptive Thau observer, in: 2013 International Conference on Unmanned Aircraft Systems (ICUAS), IEEE, 2013, pp. 550–556.
[50] P. Lu, E.J. Van Kampen, B. Yu, Actuator fault detection and diagnosis for quadrotors, in: IMAV 2014: International Micro Air Vehicle Conference and Competition 2014, Delft, The Netherlands, August 12–15, 2014, Delft University of Technology, 2014.
[51] D. Garcia, H. Moncayo, A. Perez, et al., Low cost implementation of a biomimetic approach for UAV health management, in: American Control Conference (ACC), 2016, IEEE, 2016, pp. 2265–2270.
[52] G.X. Du, Q. Quan, B. Yang, et al., Controllability analysis for multirotor helicopter rotor degradation and failure, J. Guid. Control Dyn. 38 (5) (2015) 978–985.
[53] G. Heredia, A. Ollero, M. Bejar, et al., Sensor and actuator fault detection in small autonomous helicopters, Mechatronics 18 (2) (2008) 90–99.
[54] P. Lu, E.J. van Kampen, C. de Visser, et al., Nonlinear aircraft sensor fault reconstruction in the presence of disturbances validated by real flight data, Control Eng. Pract. 49 (2016) 112–128.
[55] A. Ansari, D.S. Bernstein, Aircraft sensor fault detection using state and input estimation, in: American Control Conference (ACC), 2016, IEEE, 2016, pp. 5951–5956.
[56] G. Yun-hong, Z. Ding, L. Yi-bo, Small UAV sensor fault detection and signal reconstruction, in: Proceedings 2013 International Conference on Mechatronic Sciences, Electric Engineering and Computer (MEC), IEEE, 2013, pp. 3055–3058.
[57] K. Rudin, G.J.J. Ducard, R.Y. Siegwart, A sensor fault detection for aircraft using a single Kalman filter and hidden Markov models, in: IEEE Conference on Control Applications (CCA), IEEE, 2014, pp. 991–996.
[58] A. Abbaspour, P. Aboutalebi, K.K. Yen, et al., Neural adaptive observer-based sensor and actuator fault detection in nonlinear systems: application in UAV, ISA Trans. (2016).
[59] F.R. Lopez-Estrada, J.C. Ponsart, D. Theilliol, et al., Robust sensor fault diagnosis and tracking controller for a UAV modelled as LPV system, in: 2014 International Conference on Unmanned Aircraft Systems (ICUAS), IEEE, 2014, pp. 1311–1316.
[60] F. Caliskan, C. Hajiyev, Active fault-tolerant control of UAV dynamics against sensor–actuator failures, J. Aerosp. Eng. (2016).
[61] J. Jeong, Y. Son, J. Jung, et al., An election scheme for cooperative UAVs with fault tolerance, Adv. Sci. Technol. Lett. 110 (2015) 79–82.
[62] Z. Birnbaum, A. Dolgikh, V. Skormin, et al., Unmanned aerial vehicle security using behavioral profiling, in: 2015 International Conference on Unmanned Aircraft Systems (ICUAS), IEEE, 2015, pp. 1310–1319.
[63] S. Bhattacharya, T. Başar, Game-theoretic analysis of an aerial jamming attack on a UAV communication network, in: Proceedings of the 2010 American Control Conference, IEEE, 2010, pp. 818–823.
[64] S. Bhattacharya, Differential game-theoretic approach for spatial jamming attack in a UAV communication network, in: 14th International Symposium on Dynamic Games and Applications, 2010.
[65] J. Kim, B.H. Cho, State-of-charge estimation and state-of-health prediction of a Li-ion degraded battery based on an EKF combined with a per-unit system, IEEE Trans. Veh. Technol. 60 (9) (2011) 4249–4260.
[66] A. Barre, B. Deguilhem, S. Grolleau, et al., A review on lithium-ion battery ageing mechanisms and estimations for automotive applications, J. Power Sources 241 (2013) 680–689.
[67] M. Charkhgard, M. Farrokhi, State-of-charge estimation for lithium-ion batteries using neural networks and EKF, IEEE Trans. Ind. Electron. 57 (12) (2010) 4178–4187.
[68] S. Sepasi, R. Ghorbani, B.Y. Liaw, Improved extended Kalman filter for state of charge estimation of battery pack, J. Power Sources 255 (2014) 368–376.
[69] J. Zhang, J. Lee, A review on prognostics and health monitoring of Li-ion battery, J. Power Sources 196 (15) (2011) 6007–6014.
[70] K. Goebel, B. Saha, A. Saxena, et al., Prognostics in battery health management, IEEE Instrum. Meas. Mag. 11 (4) (2008) 33.
[71] H. Rahimi-Eichi, U. Ojha, F. Baronti, et al., Battery management system: an overview of its application in the smart grid and electric vehicles, IEEE Ind. Electron. Mag. 7 (2) (2013) 4–16.
[72] B. Saha, E. Koshimoto, C.C. Quach, et al., Battery health management system for electric UAVs, in: Aerospace Conference, 2011, IEEE, 2011, pp. 1–9.
[73] B. Bethke, J.P. How, J. Vian, Group health management of UAV teams with applications to persistent surveillance, in: 2008 American Control Conference, IEEE, 2008, pp. 3145–3150.
[74] M. Valenti, B. Bethke, J.P. How, et al., Embedding health management into mission tasking for UAV teams, in: American Control Conference, 2007, pp. 5777–5783.
[75] H.A. Izadi, Y. Zhang, B.W. Gordon, Fault tolerant model predictive control of quad-rotor helicopters with actuator fault estimation, Proc. 18th IFAC World Congr. 18 (1) (2011) 6343–6348.
[76] I. Sadeghzadeh, Y.M. Zhang, A review on fault-tolerant control for unmanned aerial vehicles (UAVs), in: Infotech@ Aerospace, St. Louis, MO, 2011.
[77] A. Chamseddine, D. Theilliol, Y.M. Zhang, C. Join, C.A. Rabbath, Active fault-tolerant control system design with trajectory re-planning against actuator faults and saturation: application to a quadrotor unmanned aerial vehicle, Int. J. Adapt. Control Signal Process. 29 (1) (2015) 1–23.
[78] M. Braun, M. Golubitsky, Differential Equations and Their Applications, Springer, New York, 1983, pp. 343–350.
[79] N.M. Vichare, M.G. Pecht, Prognostics and health management of electronics, IEEE Trans. Compon. Packag. Technol. 29 (1) (2006) 222–229.
[80] H. Beigi, R. Betti, L. Balsamo, 2014, U.S. Patent Application No. 14/297,595.
[81] Y. Zhang, X.R. Li, Detection and diagnosis of sensor and actuator failures using IMM estimator, IEEE Trans. Aerosp. Electron. Syst. 34 (4) (1998) 1293–1313.
[82] S. Zhao, B. Huang, F. Liu, Fault detection and diagnosis of multiple-model systems with mismodeled transition probabilities, IEEE Trans. Ind. Electron. 62 (8) (2015) 5063–5071.

[83] Y. Zhou, D. Wang, H. Huang, J. Li, L. Yi, Fuzzy Logic Based interactive Multiple Model Fault Diagnosis for PEM Fuel Cell Systems, INTECH Open Access Publisher., 2011.
[84] M. Compare, P. Baraldi, P. Turati, E. Zio, Interacting multiple-models, state augmented particle filtering for fault diagnostics, Probab. Eng. Mech. 40 (2015) 12–24.
[85] N. Tudoroiu, E. Sobhani-Tehrani, K. Khorasani, Interactive bank of unscented Kalman filters for fault detection and isolation in reaction wheel actuators of satellite attitude control system, in: IECON 2006—32nd Annual Conference on IEEE Industrial Electronics, IEEE, 2006, pp. 264–269.
[86] D. Jeon, Y. Eun, Distributed asynchronous multiple sensor fusion with nonlinear multiple models, Aerosp. Sci. Technol. 39 (2014) 692–704.
[87] V.P. Jilkov, X.R. Li, Online Bayesian estimation of transition probabilities for Markovian jump systems, IEEE Trans. Signal Process. 52 (6) (2004) 1620–1630.
[88] C.E. Seah, I. Hwang, Stochastic linear hybrid systems: modeling, estimation, and application in air traffic control, IEEE Trans. Control Syst. Technol. 17 (3) (2009) 563–575.
[89] H.A. Blom, Y. Bar-Shalom, The interacting multiple model algorithm for systems with Markovian switching coefficients, IEEE Trans. Autom. Control 33 (8) (1988) 780–783.
[90] L.M. Bujorianu, Applications of stochastic reachability, in: Stochastic Reachability Analysis of Hybrid Systems, Springer, London, 2012, pp. 203–207.